Journal of Magnetic Resonance 194 (2008) 237–244

Contents lists available at ScienceDirect

Journal of Magnetic Resonance

journal homepage: www.elsevier.com/locate/jmr

The utility of phase alternated pulses for the measurement of dipolar couplings in 2D-SLF experiments

Bibhuti B. Das [a], N. Sinha [b], K.V. Ramanathan [c,*]

[a] Department of Physics, Indian Institute of Science, Bangalore 560 012, India
[b] Center for Bio-Medical Magnetic Resonance, SGPGIMS Campus, Raebareli Road, Lucknow 226 014, India
[c] NMR Research Center, Indian Institute of Science, Bangalore 560 012, India

ARTICLE INFO

Article history:
Received 19 April 2008
Revised 11 July 2008
Available online 17 July 2008

Keywords:
Solid State NMR
CP
SLF
Magic-sandwich
Amplitude time averaged nutation

ABSTRACT

The measurement of hetero-nuclear dipolar coupling using two-dimensional separated local field (SLF-2D) NMR experiments is a powerful technique for the determination of the structure and dynamics of molecules in the solid state and in liquid crystals. However, the experiment is sensitive to a number of factors such as the Hartmann–Hahn match condition, proton frequency off-set and rf heating. It is shown here that by the use of phase alternated pulses during spin-exchange the effect of rf mismatch on the dipolar coupling measurement can be compensated over a wide range of off-sets. Phase alternation together with time and amplitude modulation has also been considered and incorporated into a pulse scheme that combines spin exchange with homonuclear spin decoupling based on magic sandwich sequence and named as SAMPI4. Such time and amplitude averaged nutation experiments use relatively low rf power and generate less sample heating. One of these schemes has been applied on liquid crystal samples and is observed to perform well and yield spectra with high resolution.

1. Introduction

Separated local field (SLF) spectroscopy [1] based on the transient oscillations [2] observed during cross-polarization forms a class of 2D solid state NMR experiments that have been used extensively for the estimation of dipolar couplings between the hetero-nuclei in static oriented systems. Here, the hetero-nuclear dipolar coupling is resolved from the chemical shift in an orthogonal dimension and the experiment provides a high-resolution NMR spectrum which is highly useful for the elucidation of spatial distance information between the hetero-nuclei and the orientation of internuclear vector with respect to the external magnetic field. The measured dipolar couplings can be used for building the 3D structure of molecules in the solid state [3]. However, the accuracy of the dipolar couplings determined depends on several experimental conditions. For example, for accurate estimation of the dipolar couplings, the technique requires exact Hartmann–Hahn (H–H) match during cross-polarization. Due to rf inhomogeneity and amplifier instability [4], attaining exact Hartmann–Hahn (H–H) match could prove to be difficult. Further at high magnetic fields the chemical shift dispersion is large and hence H–H matching is difficult over the entire frequency range. Such problems have been considered earlier by Shekar et al. who have utilized the off-set effects for lowering the radio frequency power input into the X-channel [5,6]. Improved pulse schemes that provide more accurate values of the dipolar couplings over a broad range of proton frequency off-sets have also been proposed [7,8]. To overcome similar problems, phase alternation techniques have been proposed earlier and improved efficiency reported in various NMR experiments. For example, the MOIST experiment [9] uses phase alternated pulses to increase the efficiency of cross-polarization. Phase alternation is a part of frequency switched Lee–Goldburg (FSLG) decoupling [10] which provides better suppression of homo-nuclear dipolar coupling during spin exchange period in PISEMA [11]. The effect of Hartmann–Hahn mismatch in PISEMA has been reported earlier by Fu et al. [4] who have considered the effect of the mismatch on the scaling factor for the PISEMA experiment. Recently, an SLF experiment incorporating the well known magic-sandwich pulses [12,13] modified for the purpose of CP transfer while at the same time ensuring homonuclear decoupling and named as SAMPI4 has been reported [14]. The experiment includes a simple combination of phase alternated pulses to overcome the effects of off-set dependence in these experiments and provides uniform line-width and intensity for all carbons over a broad spectral range.

In this paper, we consider the evolution of dipolar oscillation under phase alternation (DOPA) and show how phase alternation compensates the effect of the H–H mismatch in the basic 2D-SLF experiment. The analytical results obtained are in agreement with simulation and experiment. Yet another problem associated with the SLF experiments is the use of high power rf pulses on both channels that leads to sample heating. A solution to this problem

* Corresponding author.
E-mail address: kvr@nrc.iisc.ernet.in (K.V. Ramanathan).

1090-7807/$ - see front matter © 2008 Elsevier Inc. All rights reserved.
doi:10.1016/j.jmr.2008.07.010

is the use of time averaged precession [15], which uses unequal time periods of phase alternation to control the nutation frequency of proton magnetization. This is done in such a way that the rf requirement on the X-channel is reduced dramatically to match the Hartmann–Hahn condition. Along with time averaging, one may also use amplitude modulation for this purpose. These methods have been incorporated in PISEMA pulse sequence earlier with a considerable reduction of rf power in the observe nucleus channel [16–19]. We have incorporated the above phase alternated pulse technique for the case of the SAMPI4 experiment and observe that the method works satisfactorily even with very low rf power on the X-channel. We have utilized this modified pulse sequence to obtain high-resolution spectra for liquid crystalline samples that are observed to be sensitive to rf heating effects.

2. Dipolar oscillation under phase alternation (DOPA)

Fig. 1A shows the basic pulse sequence for the SLF experiment modified to include phase alternation on both the I and S channels at the end of every τ period. The polarization transfer dynamics under this pulse sequence can be understood following the treatment of Levitt et al. [9,20]. After the first 90° pulse, the I spin magnetization of an isolated two-spin system evolves under the Hamiltonian given in the doubly rotating tilted frame by

$$\boldsymbol{H} = \omega_{1I} I_z + \omega_{1S} S_z + 2dI_x S_x \tag{1}$$

where ω_{1I} and ω_{1S} are the applied rf fields on I and S spins, respectively, and d is the hetero-nuclear dipolar coupling constant.

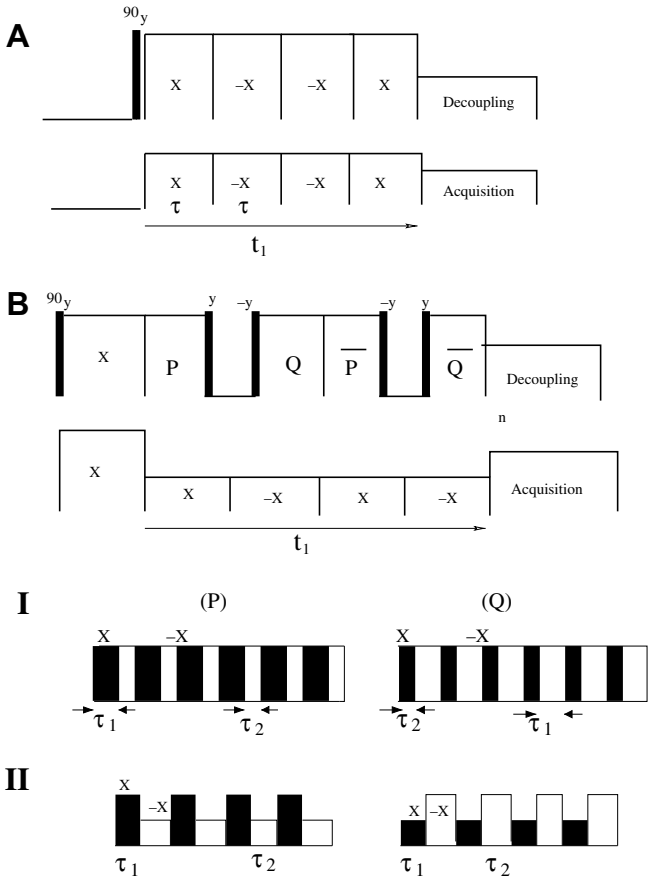

Fig. 1. Pulse sequences used in the experiments. (A) Dipolar oscillation under phase alternation (DOPA), (B) SAMPI4. (I) and (II) represent the TAN and ATAN pulses used with the pulse schemes shown in (A) and (B).

This Hamiltonian, can be represented in the zero ($\triangle$) and the double (Σ) quantum sub-spaces as follows [9]

$$\boldsymbol{H} = \boldsymbol{H}^{\triangle} + \boldsymbol{H}^{\Sigma} \tag{2}$$

$$\boldsymbol{H}^{\triangle} = (\omega_{1I} - \omega_{1S}) I_z^{\triangle} + dI_x^{\triangle}, \quad \boldsymbol{H}^{\Sigma} = (\omega_{1I} + \omega_{1S}) I_z^{\Sigma} + dI_x^{\Sigma} \tag{3}$$

with

$$I_z^{\triangle} = \frac{1}{2}(I_z - S_z), \quad I_z^{\Sigma} = \frac{1}{2}(I_z + S_z) \tag{4}$$

and

$$I_x^{\triangle} = \frac{1}{2}(I^+S^- + I^-S^+), \quad I_x^{\Sigma} = \frac{1}{2}(I^+S^+ + I^-S^-) \tag{5}$$

The initial density matrix immediately after the 90° pulse on the I spin and just before the contact pulses can be described as,

$$\tilde{\boldsymbol{\sigma}}(\mathbf{0}) = I_z = I_z^{\Sigma} + I_z^{\triangle}, \tag{6}$$

As the Hamiltonians in the zero and the double quantum frames commute with each other it is possible to calculate the evolution of the density matrix separately in both the frames which is given by,

$$\tilde{\boldsymbol{\sigma}}(\boldsymbol{t}) = \exp(-\mathrm{i}\boldsymbol{H}t)\tilde{\boldsymbol{\sigma}}(\mathbf{0})\exp(\mathrm{i}\boldsymbol{H}t) = \tilde{\boldsymbol{\sigma}}_{\boldsymbol{\Sigma}}(\boldsymbol{t}) + \tilde{\boldsymbol{\sigma}}_{\triangle}(\boldsymbol{t}) \tag{7}$$

After the spin evolution during the contact period the detectable S spin magnetization is measured as,

$$\langle S_z(t)\rangle = \mathrm{Tr}[S_z \bigstar \tilde{\boldsymbol{\sigma}}(\boldsymbol{t})] = \mathrm{Tr}[S_z \bigstar \tilde{\boldsymbol{\sigma}}_{\boldsymbol{\Sigma}}(\boldsymbol{t})] + \mathrm{Tr}[S_z \bigstar \tilde{\boldsymbol{\sigma}}_{\triangle}(\boldsymbol{t})] \tag{8}$$

With mismatched rf pulses during cross-polarization, the S spin signal intensity is calculated as

$$\langle S_z(t)\rangle = \left[\frac{(\omega_{1I}+\omega_{1S})^2}{(\omega_e^{\Sigma})^2} - \frac{(\omega_{1I}-\omega_{1S})^2}{(\omega_e^{\triangle})^2} + \frac{d^2\cos(\omega_e^{\Sigma}t)}{(\omega_e^{\Sigma})^2} - \frac{d^2\cos(\omega_e^{\Delta}t)}{(\omega_e^{\Delta})^2}\right] \tag{9}$$

where

$$\omega_e^{\Delta} = \sqrt{(\omega_{1I}-\omega_{1S})^2 + d^2} \tag{10}$$

and

$$\omega_e^{\Sigma} = \sqrt{(\omega_{1I}+\omega_{1S})^2 + d^2}. \tag{11}$$

For large rf fields, the first and third terms of Eq. (9) can be taken to be one and zero, respectively. At exact Hartmann–Hahn match ($\omega_{1I} = \omega_{1S}$), $\omega_e^{\Delta} = d$ and the magnetization oscillates with a frequency equal to the hetero-nuclear dipolar coupling given by,

$$\langle S_z(t)\rangle = 1 - \cos(dt) \tag{12}$$

In a 2D experiment where the above cross-polarization process constitutes the t_1 period, the first (constant) term on Fourier transformation gives rise to the zero frequency axial-peak [21]. The second oscillatory term gives rise to the cross-peak at the dipolar coupling frequency at Hartmann–Hahn match. Away from match, the oscillation frequency increases on either side and gives rise to error in the measurement of the dipolar coupling and to line-broadening due to rf inhomogeneity. With phase alternation, we show below that the measurement is very much less sensitive to rf mismatch. Phase alternation during t_1 is carried out as shown in Fig. 1A by periodically reversing the phase of rf pulses on both the channels at the end of every time period τ, so that the Hamiltonian during two consecutive time periods is given by

$$\boldsymbol{H}^a = \Delta\omega I_z^{\triangle} + dI_x^{\triangle} \tag{13}$$

$$\boldsymbol{H}^b = -\Delta\omega I_z^{\triangle} + dI_x^{\triangle} \tag{14}$$

where $\Delta\omega = \omega_{1S} - \omega_{1I}$. Here evolution in the zero quantum frame only is considered. Application of the average Hamiltonian theory in the zeroth order gives

$$\widetilde{\boldsymbol{H}}^{\circ} = (1/\tau_c)[\boldsymbol{H}^a\tau + \boldsymbol{H}^b\tau] \quad \text{with} \quad \tau_c = 2\tau \tag{15}$$

$$= d\boldsymbol{I}_x^{\Delta} \tag{16}$$

This indicates that the nutation frequency is independent of the mismatch in the zeroth order. An analytical expression for the oscillation frequency can also be obtained as follows. Hamiltonians shown in Eqs. (13) and (14) give rise to nutation around effective fields which are inclined to the $+x$-axis by angles $+\theta$ and $-\theta$ given by $\tan\theta = \frac{\Delta\omega}{d}$. The nutation angles during consecutive time periods are the same given by $\beta_a = \beta_b = \omega_e^{\Delta}\tau$. These consecutive nutations lead to an effective total nutation by angle β_{ab} about an axis located in the xy-plane such that [22]

$$\cos\beta_{ab} = \cos^2(\omega_e\tau/2) - \sin^2(\omega_e\tau/2)\frac{d^2 - \Delta\omega^2}{d^2 + \Delta\omega^2} \tag{17}$$

The effective dipolar oscillation frequency is therefore given by

$$\nu_{ab} = \frac{1}{2\pi\tau}\cos^{-1}\left[\cos^2(\omega_e\tau/2) - \sin^2(\omega_e\tau/2)\frac{(d^2 - \Delta\omega^2)}{(d^2 + \Delta\omega^2)}\right] \tag{18}$$

The variation of the dipolar oscillation frequency as a function of mismatch without and with phase alternation can be obtained from Eqs. (10) and (18), respectively. These plots as well as experimental results presented below demonstrate the efficacy of the DOPA (dipolar oscillation with phase alternation) experiment for removing rf mismatch dependence of measured dipolar couplings in CP-SLF experiments.

For the CP-SLF and DOPA experiments, the proton–carbon two-spin system provided by ^{13}C labeled chloroform oriented in a liquid crystal matrix has been utilized. Fig. 2A shows a cross-section of the SLF-2D spectrum obtained with the DOPA pulse sequence. The splitting of 7 kHz between the outer two lines corresponds to $J + 2d$, where J and d are the hetero-nuclear indirect spin–spin and direct dipolar couplings, respectively. Fig. 2B shows the corresponding simulated spectrum obtained by using the SIMPSON software package. The weak inner doublet observed in the spectrum arises from the double quantum part of the initial density matrix and is found to vanish both in experiment and in simulation if the system is prepared with only the zero-quantum density matrix before spin exchange begins.

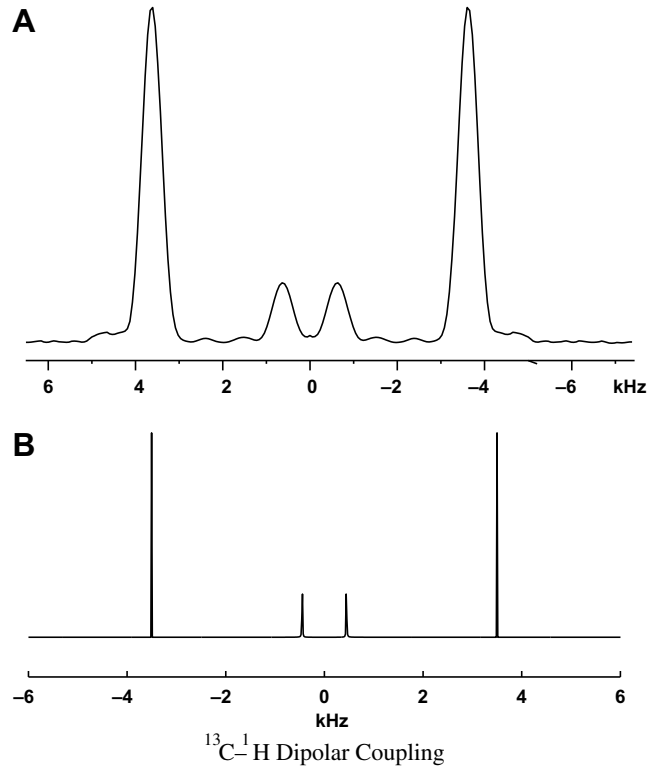

Fig. 2. (A) Dipolar cross-section of $^{13}CHCl_3$ obtained from SLF-2D experiment performed using the pulse scheme shown in Fig. 1A. (B) Simulation result for a two-spin system with a dipolar coupling constant of 3.5 kHz, for DOPA pulse scheme obtained using SIMPSON programing package.

A comparison of the performance of DOPA with respect to simple CP-SLF is presented in Fig. 3. Fig. 3A–D corresponds to the CP-SLF spectra of chloroform with the rf mismatch varying from 6 to 0 kHz. Fig. 3E–H corresponds to the DOPA spectra over the same range of rf mismatch. As seen in the spectra the dipolar cross-peaks shows very little variation with rf mismatch for DOPA while in the SLF spectra they vary significantly, as a function of $\Delta\omega$. Fig. 3 also shows the plot of dipolar couplings as a function of mismatch obtained from Eqs. (10) and (18). The dotted line in the figure corresponds to CP-SLF and the solid line to DOPA experiments. The CP-SLF experiment shows a parabolic variation of the measured dipolar couplings as a function of the measured dipolar couplings as a function of mismatch, while the DOPA result corresponds to an almost flat profile. The insensitivity to rf mismatch of the DOPA sequence has two advantages: (a) the measurement provides accurate dipolar couplings, independent of rf mismatch; (b) the measurement is also insensitive to rf inhomogeneity effects, which otherwise would broaden the line and shorten the duration of the dipolar oscillations due to the spread of apparent dipolar couplings.

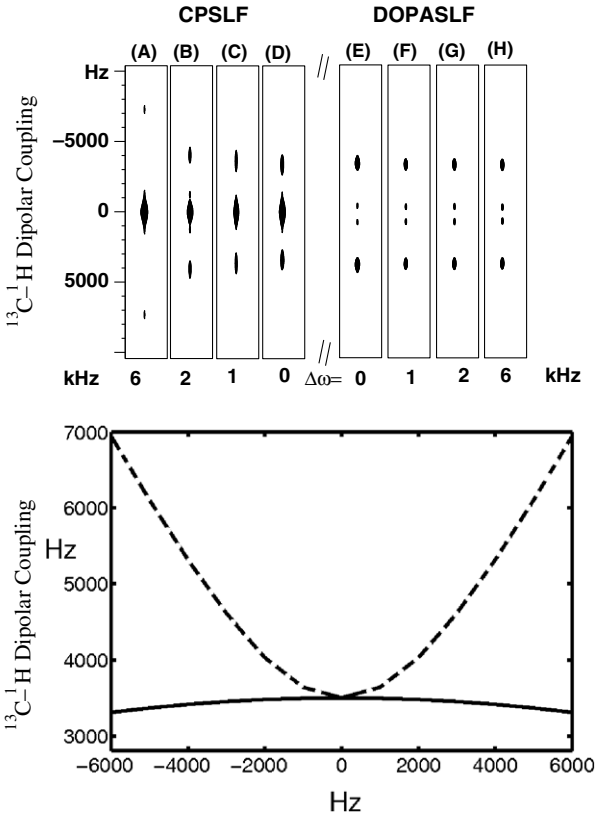

Fig. 3. (Top) Experimental SLF-spectra of chloroform under various mismatch conditions. (A)–(D) correspond to CP-SLF experiments acquired under rf mismatch of 0, 1, 2 and 6 kHz. (E)–(H) correspond to SLF spectra obtained using DOPA pulse scheme for rf mismatch of 0, 1, 2 and 6 kHz. (Bottom) Graph showing change in dipolar coupling with respect to the rf mismatch corresponding to Eq. (18) (dotted line) and Eq. (10) (solid line). Dipolar coupling constant was set to 3.5 kHz and rf mismatch ($\Delta\omega$) was changed from −6 to 6 kHz.

In the section below phase alternation together with the use of time and amplitude modulation is considered. These features have been incorporated into SLF experiments which use the magic sandwich pulses for homo-nuclear decoupling. The modified pulse sequences are found to work efficiently with low rf power thereby reducing problems associated with sample heating.

3. Phase alternation and time and amplitude averaged nutation

One of the problems of 2D SLF experiments is that the rf used during the spin-lock period tends to heat up the sample. A solution proposed for reducing the rf power required for the S nucleus for achieving Hartmann–Hahn match has been the use of time averaged nutation [15]. This has been incorporated into LG-CP and PISEMA experiments [16,17,19,18] where the power requirement is even higher for the S spin as it has to match the effective field on proton arising from rf applied away from resonance to satisfy the Lee–Goldburg condition [23]. Another pulse sequence for the SLF experiment proposed recently has on-resonance rf both for I and S spins and uses the Magic-Sandwich pulses for achieving homo-nuclear decoupling [14]. This sequence named as SAMPI4 has been further modified to include homo-nuclear decoupling on the S spin also and is referred to as MS-2 [24]. We have considered here the use of time averaged nutation (TAN) and amplitude time averaged nutation (ATAN) for the above SLF pulse sequences for the purpose of reducing the rf power. We have also applied the modified sequences to obtain the SLF-2D spectrum of a liquid crystalline sample found to be sensitive to sample heating.

Time and amplitude averaged experiments essentially utilize phase alternated pulse sequences with unequal duration of phase alternation, such that the overall nutation frequency over one cycle is a fraction of the nutation frequency corresponding to the rf applied. The TAN and ATAN pulse sequences are shown in Fig. 1 as insets I and II, respectively. In the TAN sequence one cycle of period τ_c consists of two time periods τ_1 and τ_2 with the phase altered by 180° between the two periods. These pulses applied on the I spin, reduce the I spin average nutation frequency by the time averaging factor,

$$\mathrm{TAF} = \frac{\tau_1 - \tau_2}{\tau_c}, \tag{19}$$

where

$$\tau_c = \tau_1 + \tau_2. \tag{20}$$

The rf nutation frequency for the S spin for achieving Hartmann–Hahn match is reduced by the same factor. The ATAN experiment is similar to TAN with the phases of the rf during τ_1 and τ_2 periods being opposite of each other. In addition, the rf amplitude are also unequal so that the Hartmann–Hahn condition is given by

$$\frac{(\omega_{1I})_1\tau_1 - (\omega_{1I})_2\tau_2}{\tau_c} = \omega_{1S}. \tag{21}$$

The advantage of the ATAN pulse sequence is that the average rf power applied not only to the S spin, but also to the I spin is reduced. Both in the TAN and the ATAN experiments, the number of such pulse pairs are adjusted to be such that an effective nutation angle of 360° for the spin is achieved. This forms a super cycle denoted by P. Subsequently, all the phases are reversed as shown in Fig. 1 to form the counter rotating super cycle denoted by Q. Correspondingly the phases on the S spin during P and Q are also reversed which ensures evolution under dipolar coupling while off-set effects are nullified. However, as pointed by Nishimura and Naito [17], the use of the TAN and ATAN pulse sequences produce an additional scaling of the dipolar coupling arising from the fact that the time averaging for the hetero-nuclear dipolar coupling is different under the phase and amplitude modulated pulse sequences used. Analytical expressions for the scaling factor are also available. Here we have estimated these scaling factors experimentally and by simulation for TAN and ATAN experiments.

The TAN and ATAN modifications have been introduced into the DOPA pulse sequence shown in Fig. 1A. The following experiments were carried out with the parameters and results as summarized below:

(i) *ATAN-DOPA*: RF amplitudes in the ratio $\omega_{1I} : \frac{2}{3}\omega_{1I}$ and $\tau_1 = \tau_2$. This gives a TAF = 1/6. This means that $\omega_{1S} = \frac{\omega_{1I}}{6}$ is sufficient for achieving Hartmann–Hahn match. The experimental result for oriented $^{13}CHCl_3$ is shown in Fig. 4A and the result of simulation is shown in Fig. 4D. The dipolar coupling is scaled by 0.8 in this case.

(ii) *ATAN-DOPA*: RF amplitudes in the ratio $\omega_{1I} : \frac{1}{2}\omega_{1I}$, $\tau_1 = \tau_2$ and TAF = 1/4. Experimental and simulation results shown in Fig. 4B and E, respectively. The dipolar scaling factor = 0.73.

(iii) *TAN-DOPA*: $\tau_1 = 5.3$ μs and $\tau_2 = 2.7$ μs. TAF = 0.325. Experimental and simulation results are shown in Fig. 4C and F, respectively. The scaling factor is 0.7.

As evident from the foregoing discussion the rf amplitude on the X-channel required for spin-locking the S spin for Hartmann–Hahn match is significantly reduced by adopting the TAN and

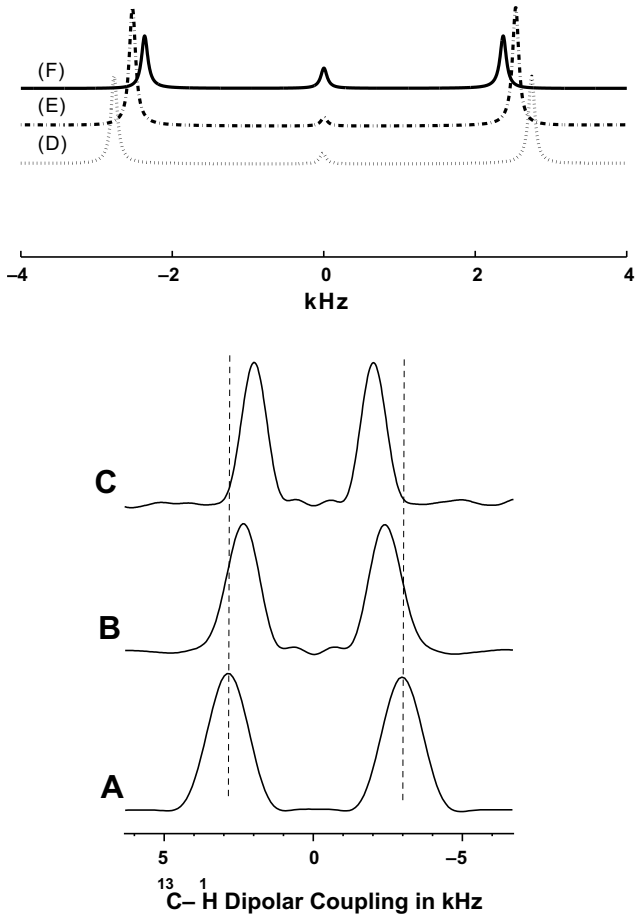

Fig. 4. Simulation and experimental results for a two-spin system obtained for the DOPA pulse sequence with the incorporation of TAN and ATAN concepts. Experimental (A and B) and simulation (D and E) results obtained for the ATAN-DOPA scheme with the rf power on the proton channel switched between 62.5 and 31 kHz. (A) and (D) correspond to rf-power switched between 62.5 and 31 kHz. (B) and (E) correspond to rf power switched between 62.5 and 41 kHz. (C) Experiment and (F) simulation results for TAN-DOPA pulse sequence with the time modulation periods $\tau_1 = 5.3$ μs and $\tau_2 = 2.7$ μs. Experiments were carried out with t_1 evolution up to 1.5 ms for ATAN-DOPA and 2.2 ms for TAN-DOPA, respectively.

ATAN approaches. Consequently, the rf power which varies as the square of the rf amplitude is also considerably reduced and this should be beneficial for obtaining the spectra of heat sensitive samples.

4. SAMPI4 with amplitude time averaged nutation

In the experiments described in the previous section, homo-nuclear dipolar decoupling has not been used. However, for practical utility, it is necessary to employ homo-nuclear decoupling as otherwise the dipolar oscillations are severely damped. PISEMA [11] utilizes Lee–Goldburg decoupling [23] for this purpose. Recently, a new CP-SLF experiment named as SAMPI4 has been proposed [14] which employs the magic sandwich sequence [12] for homo-nuclear decoupling. This pulse sequence has the advantage that unlike PISEMA it employs on resonance rf during spin exchange. As a result, the power requirement on the X-nucleus channel for Hartmann–Hahn match is significantly less than what is required for PISEMA. It also has certain other advantages such as better tolerance to proton-frequency off-sets and more uniform line-width and intensities over the full spectral range. The rf requirement of this pulse sequence can further be reduced by applying the concept of time averaged nutation. Of the three experiments described in the previous section, we have utilized

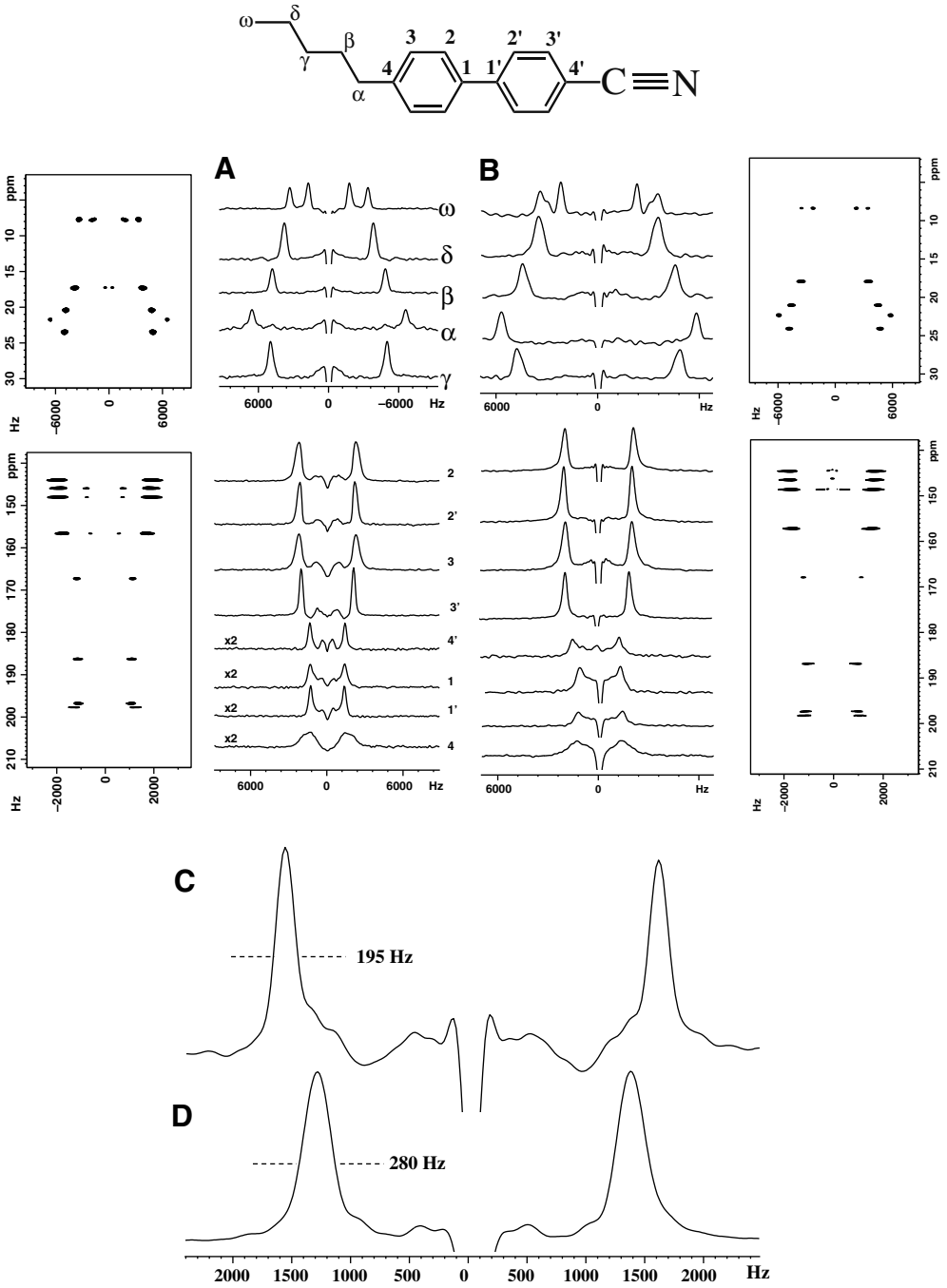

Fig. 5. 2D-spectra with dipolar cross-sections of aliphatic and aromatic carbons in 5CB. Experiments for (A) ATAN-SAMPI4 and (B) ATAN-SEMA were carried out for dwell times of 60 and 105 μs. 3 ms polarization inversion contact pulses with radio frequency of 62.5 kHz were used for CP in both the experiments. (C) and (D) Comparison of line widths for dipolar cross-section of $C_{3'}$ obtained for ATAN-SAMPI4 and ATAN-SEMA, respectively. During t_1 evolution under ATAN pulses, the rf power on X-channel was decreased to 15 kHz in ATAN-SAMPI4, where as for ATAN-SEMA the rf power was set at 19 kHz. Two transients with 20 s recycle delay were used for each t_1 increment.

the conditions corresponding to the first experiment which an ATAN sequence is providing the lowest time averaged nutation factor and the highest scaling factor. The pulse sequence is shown in Fig. 1B. The experiments have been carried out on a static oriented liquid crystal sample of 4-pentyl-4′-cyanobiphenyl (5CB). The results of the ATAN-SAMPI4 experiment are presented in Fig. 5A. For comparison, experiments were also carried out using the ATAN-SEMA pulse sequence using LG decoupling for homo-nuclear decoupling. These results are shown in Fig. 5B. Both the experiments were carried with an initial contact period of 3 ms with both proton and carbon rf fields of 62.5 kHz for polarization inversion. During spin exchange the amplitude of proton rf was switched between 62.5 and 31 kHz over equal time periods ($\tau_1 = \tau_2$) of 4 μs for SAMPI4 and 6.5 μs for PISEMA. The dwell times were 60 and 105 μs for the two experiments. This required the use of 15 and 19 kHz for the X-channel, respectively, for the ATAN-SAMPI4 and ATAN-SEMA experiments. From Fig. 5A and B it may be concluded that in general the performance of ATAN-SAMPI4 and ATAN-SEMA are comparable. Close examination of the spectra reveal a few features which highlight the advantage of the SAMPI4 experiment. For example, the ATAN-SAMPI4 experiment gives uniform line-width for all the carbon chemical sites in comparison to the ATAN-SEMA experiment as evident from the line-width and resolution for the methyl and the quaternary carbons. The axial peaks are also less intense. This also compares well with the line-width of more than 250 Hz obtained with the SAMPI4 sequence without the ATAN modification. This may be attributed to better temperature stability in the ATAN experiment due to low rf power used as discussed further in the next section. The scaling factor in the case of ATAN-SAMPI4 is also higher at 0.9, compared to 0.6 for the ATAN-SEMA experiment. Fig. 5C and D compares the line-width of one of the aromatic carbons (C_3-carbon) for the two experiments. ATAN-SAMPI4 provides a line-width 195 Hz for this carbon in comparison to 280 Hz obtained from the ATAN-SEMA experiment. The scaling factor in the case of SAMPI4 is also higher at 0.9, compared to 0.6 for the SEMA experiment.

The effect of proton carrier frequency offset for the ATAN-SAMPI4 and ATAN-SEMA experiment have also been investigated and the results for the C_3 carbon are shown in Fig. 6 for off-sets up to 6 kHz. It is observed that for ATAN-SAMPI4 the changes in line width, intensity and the measured value of the dipolar couplings are not significant for an off-set of 3 kHz, while at 6 kHz the changes in the above quantities are just beginning to be visible. On the other hand, for the ATAN-SEMA experiment for an off-set of 3 kHz the dipolar splitting increases significantly, the cross-peaks broaden and the intensity drops significantly. At 6 kHz the cross-peaks are not visible and hence the spectrum is not shown in the figure. The off-set independence of the SAMPI4 scheme demonstrated here, arises from the phase reversals included in the pulse scheme [14,24]. Similarly, the pulse scheme is expected to be less sensitive to carbon chemical shift anisotropy. This will make the method highly useful for the study of powder samples under static conditions as well as under magic angle sample spinning and at high fields and a systematic study of these aspects needs to be undertaken.

The TAN and ATAN pulse schemes proposed here tend to make the cycle times longer, because of the addition of pulses of opposite phase and the decreased nutation frequency. This has the effect of increasing the dwell time and decreasing the available spectral window. While the 60 μs dwell time used here suffices for the liquid crystal samples investigated, a larger spectral width may be necessary, say for more rigid systems such as single crystals. This can be achieved by increasing the proton rf and decreasing τ_1 and τ_2. Thus, a proton rf ratio of 100:50 kHz and a carbon rf of 25 kHz will decrease the dwell time to 37.5 μs corresponding to a spectral width of 29 kHz. However, more studies are required to understand both the decoupling efficiency and rf heating effects in such systems.

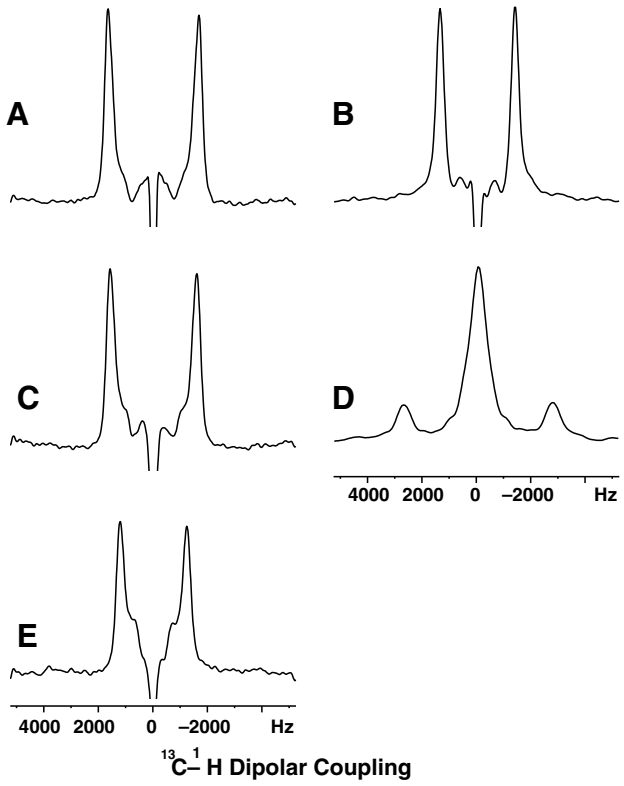

Fig. 6. Effect of frequency off-sets in proton channel obtained for ATAN-SAMPI4 (left) and ATAN-SEMA (right). The cross-sections are shown for the C_3 carbon in 5CB for experiments with off-sets of 0, 3 and 6 kHz.

Recently, the use of a proton detected PISEMA experiment that provides significant improvement in sensitivity has been proposed [25,26]. Such an experiment needs measurement windows during acquisition of the proton signals and suitably modified homonuclear decoupling sequences have been used for this purpose. In the magic sandwich pulse scheme discussed here, there is a large window of zero rf power in every decoupling cycle and this makes the SAMPI4 an attractive pulse scheme for use as a proton detected experiment.

5. Application of ATAN-SAMPI4 to a hydrogen bonding donor liquid crystal

The usefulness of pulse sequences that produce low rf heating in the process of measuring dipolar couplings is demonstrated on a three ring based calamitic mesogen. The molecular structure of the mesogen is shown in Fig. 7. It consists of three ring core with ester and azomethine linking units and hexyloxy chain at one end of the terminal. It shows nematic phase with characteristic transition temperatures at T_{C-N} −112.4 °C and T_{N-I} −155 °C [27]. The mesogen is important in view of the presence of pyridine at one end of the terminal. Building supra-molecular thermotropic liquid crystals using hydrogen bonding is gaining popularity in view of ease of synthesis and the possibility of making new devices [28]. The pre-requisite for such a process is presence of hydrogen bonding acceptor like pyridine which facilitates the formation of hydrogen bonding when appropriate donor is mixed [29].

The proton decoupled ^{13}C spectrum of this compound was recorded by employing the standard CP pulse sequence and also

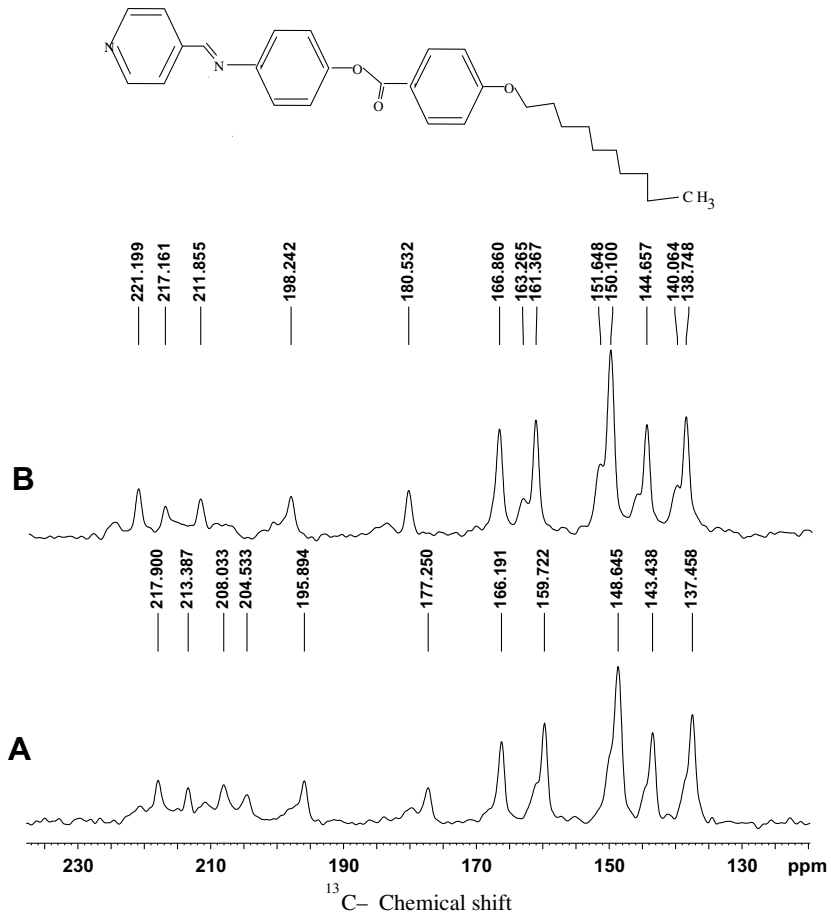

Fig. 7. 1D ^{13}C spectrum of a mesogen with pyridyl group. (A) CP spectrum obtained with 62.5 kHz rf used in both proton and carbon channels. (B) ATAN-CP spectrum acquired with the rf modulation of 62.5 kHz:31 kHz on proton channel. The rf power was decreased to 15 kHz on carbon channel for Hartmann–Hahn match. 64 scans with 3 s recycle delay were used in each experiment. SPINAL-64 decoupling of proton with 30 kHz of rf was used during the acquisition in both the experiments.

using the ATAN modification to the CP pulse sequence. In the first case the rf power on both the proton and carbon channels were 62.5 kHz. For the ATAN-CP, the ^{1}H rf was switched between 62.5 and 31 kHz during τ_1 and τ_2. The carbon rf field was kept constant at 15.5 kHz to satisfy the Hartmann–Hahn match. During the signal acquisition period of 25 ms SPINAL-64 [30] decoupling of protons was employed. The spectra of the aromatic part of the sample obtained corresponding to CP and ATAN-CP are shown in Fig. 7A and B, respectively. The spectra were recorded keeping all other conditions identical in both the cases. A relaxation delay of 3 s was used between scans and the temperature of the heating air was maintained at 418 K. However, one may notice the considerable difference in the chemical shifts up to 4 ppm of the peaks in the two spectra. This indicates that the spectrum recorded with the standard CP pulse sequence generates more heat locally due to the higher rf power used. As a result, the peaks tend to drift towards their isotropic chemical shifts. In such cases, it is advantageous to use the time averaged nutation for the proton channel. This is illustrated by the ATAN-SAMPI4 2D spectrum of the same sample shown in Fig. 8. The experimental conditions are given in the captions of the figures. The high quality of the 2D spectrum and the extremely sharp contours indicate that rf heating effects have been minimal under the condition of the experiment. The 2D spectrum shows seven contours representing six chemically inequivalent CH carbons belonging to the three rings and one CH carbon of the azomethine linking unit. Due to the different chemical environments and orientation with respect to molecular axis, the carbon chemical shifts are spread over 130–200 ppm and the dipolar coupling are in the range of 2.0–2.6 kHz for aromatic rings and 3.9 kHz for azomethine. A cross-section of the 2D-spectrum corresponding to the peak around 191 ppm is also shown in Fig. 8, which shows a line-width of only 150 Hz. Further the 2D spectrum shows two well resolved dipolar peaks around 150 ppm for two of the carbon sites whose resonances overlap in the 1D spectrum. The difference

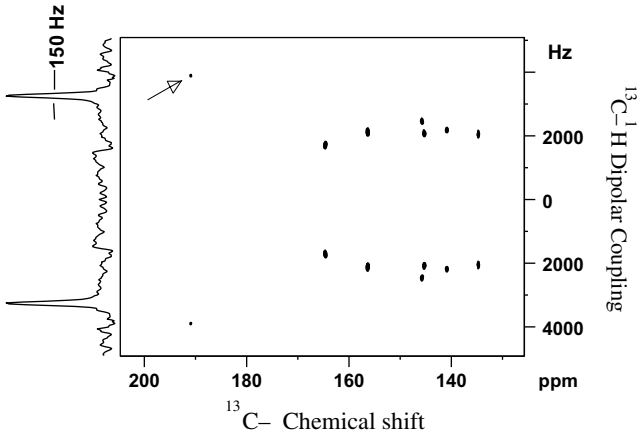

Fig. 8. SLF-2D spectrum of the mesogen with a pyridyl group. The 2D spectrum was obtained with 24 scans for each of a total of 110 t_1 increments. The dwell time for each increment was 60 μs and a total period for t_1 evolution was typically up to 6.6 ms. A 1D cross-section corresponding to the peak at 191 ppm indicated by the arrow is shown along the F_1 axis.

in the dipolar couplings between these two carbon sites is just 350 Hz. Such fine distinctions have been possible due to the improved line width provided by the experiment. The measurement of even small differences in dipolar couplings between carbons with overlapping chemical shifts is significant since it enables obtaining detailed information on the order and orientation in molecules with possible technological applications. Thus the technique promises to be of significant use for several temperature sensitive liquid crystalline systems as well as for biological samples.

6. Experiment

Experiments were carried out on ^{13}C labeled chloroform oriented in the thermotropic liquid crystal of EBBA (*N*-(*p*′-ethoxy benzylidine) *p*-*n*-butylaniline) at 310 K and on the liquid crystal 4-pentyl-4′-cyanobyphenyl (5CB) in its nematic phase. Bruker AV500 solid state FT-NMR spectrometer equipped with a 4 mm MAS probe was used to carry out the experiments under stationary conditions. The resonance frequencies were 500.17 and 125.77 for ^{1}H and ^{13}C, respectively. Radio frequency pulse strengths during cross-polarization and t_1 periods were 62.5 kHz in the ^{1}H and ^{13}C channels for DOPA experiments. The rf power on the carbon channel during spin exchange with FSLG decoupling was increased to match the effective field for protons. SPINAL64 [30] pulse scheme with an rf input of 30 kHz were used in proton channel for hetero-nuclear decoupling. Typically, in the case of DOPA experiment, 32 μs dwell time was used and 72 t_1 points were acquired along the indirect dimension. 128 t_1 data points were acquired for PISEMA and SAMPI4 experiments. Additional details of individual experiments are given in respective figure captions. Simulation results shown here were obtained using SIMPSON [31] programme.

7. Conclusion

We have considered here the utility of phase alternated pulses for 2D-SLF experiments based on Hartmann–Hahn cross-polarization. We observe that a simple modification to the basic CP-SLF experiment improves its performance in terms of its sensitivity to rf mismatch and inhomogeneity. More sophisticated modifications that include time and amplitude averaged nutation have the advantage of low rf heating of the sample. Incorporating these modifications to the SAMPI4 pulse sequence that includes the magic sandwich sequence for homo-nuclear dipolar decoupling, experiments have been carried out on liquid crystal samples. It is observed the experiments yield high quality spectra and the technique promises to be of routine use for the study of oriented liquid crystals and biological macro-molecules.

Acknowledgments

The use of AV-500 Solid State NMR Spectrometer funded by the Department of Science and Technology (DST), New Delhi, at the NMR Research Centre Indian Institute of Science, Bangalore is gratefully acknowledged. KVR acknowledges DST for a research grant for "New Methods and Techniques for Solid State NMR Spectroscopy–Rapid Data Collection and Application to Biological Systems".

References

[1] R.K. Hester, J.L. Ackerman, V.R. Cross, J.S. Waugh, Phys. Rev. Lett. 34 (1975) 993.
[2] L. Muller, A. Kumar, T. Baumann, R.R. Ernst, Phys. Rev. Lett. 32 (1974) 1402.
[3] A. Ramamoorthy, Y. Wei, D.K. Lee, Annu. Rep. NMR Spectrosc. 52 (2004) 1.
[4] R. Fu, C. Tian, H. Kim, S.A. Smith, T.A. Cross, J. Magn. Reson. 159 (2002) 167.
[5] S.C. Shekar, D.K. Lee, A. Ramamoorthy, J. Magn. Reson. A 157 (2002) 223.
[6] S.C. Shekar, D.K. Lee, A. Ramamoorthy, J. Am. Chem. Soc. 123 (2001) 7467.
[7] K. Yamamotto, D.K. Lee, A. Ramamoorthy, Chem. Phys. Lett. 407 (2005) 289.
[8] S.V. Dvinskikh, K. Yamamotto, A. Ramamoorthy, J. Chem. Phys. 125 (2006) 34507.
[9] M.H. Levitt, D. Sutar, R.R. Ernst, J. Chem. Phys. 84 (1986) 4243.
[10] A. Bielecki, A.C. Kolbert, H.J.M. de Groot, R.G. Griffin, M.H. Levitt, Adv. Magn. Reson. 14 (1990) 111.
[11] C.H. Wu, A. Ramamoorthy, S.J. Opella, J. Magn. Reson. A 109 (1994) 270.
[12] K. Takegoshi, C.A. McDowell, Chem. Phys. Lett. 116 (1985) 100.
[13] W.K. Rhim, A. Pines, J.S. Waugh, Phys. Rev. B 3 (1971) 684.
[14] A.A. Nevzorov, S.J. Opella, J. Magn. Reson. 185 (2007) 59.
[15] K. Takegoshi, C.A. McDowell, J. Magn. Reson. 67 (1986) 356.
[16] K. Nishimura, A. Naito, Chem. Phys. Lett. 380 (2003) 569.
[17] K. Nishimura, A. Naito, Chem. Phys. Lett. 402 (2005) 245.
[18] D.K. Lee, T. Narasimhaswamy, A. Ramamoorthy, Chem. Phys. Lett. 399 (2004) 359.
[19] K. Nishimura, A. Naito, Chem. Phys. Lett. 419 (2006) 120.
[20] M.H. Levitt, J. Chem. Phys. 94 (1991) 30.
[21] B.B. Das, T.G. Ajith Kumar, N. Sinha, S.J. Opella, K.V. Ramanathan, J. Magn. Reson. 185 (2007) 308.
[22] C. Counsell, M.H. Levitt, R.R. Ernst, J. Magn. Reson. 63 (1985) 133.
[23] M. Lee, W.I. Goldberg, Phys. Rev. A 140 (1965) 1261.
[24] Bibhuti B. Das, T.G. Ajith Kumar, K.V. Ramanathan, Solid State Nucl. Magn. Reson. 33 (2008) 57.
[25] C.H. Wu, S.J. Opella, J. Magn. Reson. 190 (2008) 165.
[26] C.H. Wu, S.J. Opella, J. Chem. Phys. 128 (2008) 52312.
[27] M. Paul, T. Narasimhaswamy, in: Poster Presented at the International Conference on Liquid Crystals, University of Mumbai, December 2006.
[28] T. Kato, N. Mizoshita, K. Kishimoto, Angew. Chem., Int. Ed. 45 (2006) 38.
[29] J. Lee, J. Jin, M.F. Achard, F. Hardouin, Liq. Cryst. 28 (5) (2001) 663.
[30] B.M. Fung, A.K. Khitrin, K. Ermolaev, J. Magn. Reson. 142 (2000) 97.
[31] M. Bak, J.T. Rasmussen, N.C. Nielsen, J. Magn. Reson. 147 (2000) 296.